IEEE Access
Multidisciplinary | Rapid Review | Open Access Journal

Received April 18, 2019, accepted May 12, 2019, date of publication May 24, 2019, date of current version June 19, 2019.

Digital Object Identifier 10.1109/ACCESS.2019.2918616

Adaptive Space-Frequency Equalization for SC-FDE Systems With Interference

YAN LI[1], WEILE ZHANG[1], RUIWEN JIANG[1], AND SHUN ZHANG[2]
[1]School of Electronic and Information Engineering, Xi'an Jiaotong University, Xi'an 710049, China
[2]State Key Laboratory of Integrated Services Networks, Xidian University, Xi'an 710071, China

Corresponding author: Weile Zhang (wlzhang@mail.xjtu.edu.cn)

This work was supported in part by the National Natural Science Foundation of China (NSFC) under Grant 61671366 and Grant 61601058, in part by the Natural Science Basic Research Plan in Shaanxi Province of China under Grant 2016JQ6005, and in part by the Fundamental Research Funds for the Central Universities.

ABSTRACT In this paper, we propose a new space-frequency adaptive equalization (SFAE) method for single carrier frequency domain equalization (SC-FDE) systems that can deal with multipath interference from the highly delay-dispersive channel as well as the multiuser interference. Based on the minimum mean square error (MMSE) criterion, we derive the adaptive weights by combining the received multi-antenna signals in the frequency domain. The main computation burdens of the proposed SFAE and the conventional space-time adaptive equalization (STAE) lie in the calculation of the autocorrelation matrix R and its inversion. The autocorrelation matrix in the SFAE is exactly a block Toeplitz matrix whose calculation can be efficiently implemented by the fast Fourier transformation (FFT) and its inversion also has fast algorithms. Compared with the conventional STAE method, the proposed SFAE method has comparable interference suppression performance, but with a lower order computational complexity. Hence, the proposed SFAE should be more attractive from a practical point of view. The numerical results are provided to corroborate the proposed studies.

INDEX TERMS Channel equalization, interference suppression, space-frequency filtering.

I. INTRODUCTION

There are two main kinds of interferences in wireless communication process. One is the multipath interference, which is usually tackled by employing cyclic prefix (CP) in orthogonal frequency division multiplexing (OFDM) or single carrier frequency domain equalization (SC-FDE). However, when the multipath delay spread is larger than the CP duration, i.e., in the so-called insufficient CP scenario, the receiver would suffer from both inter-block interference (IBI) and inter-carrier interference (ICI). The other is the multi-user interference. When multiple users communicate simultaneously, the interference among different links would greatly degrade wireless transmission quality.

For the multipath interference in highly delay-dispersive channel, propagation conditions in which the channel maximum excess delay exceeds the normal CP duration of $4.69\mu s$ occur infrequently but often enough to deserve attention and be accounted for in 4G/LTE [1]. During the past few years, various solutions have been proposed to suppress the multipath interference in highly delay-dispersive channel [1]–[10].

The associate editor coordinating the review of this manuscript and approving it for publication was Zhen Gao.

For example, based on Bayesian inference and sparse signal reconstruction, the authors of [1] derive an iterative algorithm that estimates an approximate representation of channel and the noise variance, which can finally cancel the intrinsic interference. In [3], a bi-directional M-algorithm (BDMA) is proposed with high-performance trellis-based equalization for scenarios with insufficient CP, which can get favorable result after only two iterations. Aiming at insufficient CP single input multiple output (SIMO)-OFDM systems, the work in [5] analyzes the effect of insufficient CP, and proposes a two-stage receiver that uses zero-forcing (ZF) or minimum mean square error (MMSE) to estimate the transmitted data to support the high performance trellis based detector. By use of the null side subcarriers and the redundancy of CP, a frequency-domain equalizer (FEQ) for OFDM systems with insufficient CP is developed in [7]. For SC-FDE with insufficient CP, the method in [8] removes the residual interference by filling the missing symbols. For SC-FDE in High Frequency (HF) wireless communications, [10] proposes an efficient estimation method for channel parameters based on the Synchronization Training Sequences (STS) structure.

Another typical approach to deal with interference based on the concept of space-time adaptive equalization (STAE) has also received a lot of research attentions [11]–[20]. It is demonstrated that the STAE can simultaneously suppress both highly delay dispersive multipath interference as well as multi-user interference. For multi-user multiple input multiple output (MIMO), the author of [11] introduces a frequency synchronization scheme based on space-time equalization, which can perform data recovery in the presence of interference. The pioneer work in [12] provides a two-stage hybrid interference cancellation and equalization framework, in which the first stage uses time-domain equalization to suppress co-channel interference while the second stage performs low-complexity single tap equalization and detection. Tang and Heath [14] propose a receiver structure that can perform joint synchronization and space-time equalization. Their work makes use of a novel space-time equalization algorithm based on the channel state information and a training-based MMSE algorithm to achieve desirable bit error rate (BER) performance. In [17], a hybrid iterative analog-digital equalizer is designed to remove the multiuser interference. Before the analog precoders, a space-time encoder is used to simplify the receiver optimization. The analog and digital parts of the hybrid iterative equalizer are designed jointly using average BER as the metric. A mean square error (MSE)-prediction scheme to adaptively determine the optimal temporal filter (TF) length in a space-time equalization (STE) is presented in [19]. Although the STAE-type schemes exhibit powerful ability of interference suppression, they involve the calculation of the high-dimensional space-time autocorrelation matrix as well as its inversion. This would be of quite high computational complexity which prohibits its application in practice.

In this paper, we propose a space-frequency adaptive equalization (SFAE) method to deal with both highly delay-dispersive channel and multiuser interference for SC-FDE systems. The received multi-antenna signals are adaptively combined in frequency domain, while the proposed adaptive weights are derived according to MMSE criterion under a time-domain constraint. It is observed that the proposed SFAE method performs basically the same as the conventional STAE method in terms of interference suppression. More importantly, it is observed that, the autocorrelation matrix in SFAE is exactly a block Toeplitz matrix whose calculation can be efficiently implemented by fast Fourier transformation (FFT) and its inversion also has fast algorithms. We can find out that the proposed SFAE has a lower order of computational burden than the conventional STAE. Therefore, the proposed SFAE should be more attractive from practical point of view.

The remainder of this paper is organized as follows. The system model is illustrated in Section II. The proposed SFAE is presented in Section III. Simulation results are provided in Section IV. Section V concludes the paper.

Notations: Superscripts $(\cdot)^*$, $(\cdot)^T$ and $(\cdot)^H$ represent conjugate, transpose and Hermitian, respectively; $\mathbb{C}^{m\times n}$ defines the vector space of all $m \times n$ complex matrices; $\|\cdot\|$ denotes the Frobenius norm operator; diag($\boldsymbol{x}$) is a diagonal matrix whose elements on main diagonal are the elements of $\boldsymbol{x}$.

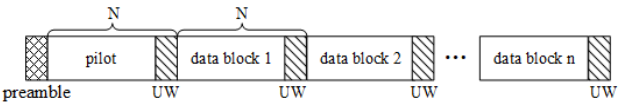

FIGURE 1. Illustration of one typical structure of SC-FDE signal frame.

II. SYSTEM MODEL

We consider a Non-Line-Of-Sight (NLOS) communication system, where the transmitting terminal is equipped with a single antenna, and the receiving terminal has M antennas. We assume the channels between the transceivers are the frequency selective Rayleigh fading propagation channels. The total channel matrix is $\mathbf{H} = [\mathbf{h}_1, \mathbf{h}_2, \cdots, \mathbf{h}_M] \in \mathbb{C}^{(L+1)\times M}$, where $\mathbf{h}_m = \left[h_m(0), h_m(1), \cdots, h_m(L)\right]^T$ denotes the channel response vector corresponding to the *mth* antenna.

We consider the burst mode transmission, where one frame is composed of one pilot block and several subsequent data blocks. In practice for purpose of automatic gain control (AGC), the frame is initialized with a short preamble. As shown in Fig. 1, we divide the transmitted data into blocks, and insert unique word (UW), which serves similarly as CP, at the end of each block.

First, we introduce the basic concept of conventional STAE. As shown in Fig. 2, STAE performs space-time adaptive filtering, where each time-domain filter has $Q+1$ tap coefficients. Denote the transmitted pilot signal as $\mathbf{s} = [s(0), s(1), \cdots s(N-1)]^T \in \mathbb{C}^{N\times 1}$. Then, in the noise-free environment, the received signal matrices with different sampling offsets are concatenated together. That yields the space-time signal matrix given in (1), as shown at the bottom of the next page. Here, $\tilde{\mathbf{s}}_i$ denotes the downward cyclic shift of pilot $\mathbf{s}$ by a factor of i samples; $\mathcal{T}(\mathbf{h}_m)$ represents the Toeplitz matrix given as below

$$\mathcal{T}(\mathbf{h}_m) = \begin{bmatrix} h_m(0) & 0 & \cdots & 0 \\ h_m(1) & h_m(0) & \ddots & \vdots \\ \vdots & \vdots & \ddots & 0 \\ h_m(L) & h_m(L-1) & \ddots & h_m(0) \\ 0 & h_m(L) & \ddots & \vdots \\ \vdots & 0 & \ddots & \vdots \\ \vdots & \vdots & \ddots & \vdots \\ 0 & 0 & \cdots & h_m(L) \end{bmatrix}. \quad (2)$$

We denote the $M(Q+1)\times 1$ space-time weighting vector by $\mathbf{w}_{ST} = \left[\mathbf{w}_1, \mathbf{w}_2, \cdots, \mathbf{w}_M\right]^T$, where $\mathbf{w}_i = \left[w_i^0, w_i^1, \cdots, w_i^Q\right]$ denotes the spatial filtering vector corresponding to the *ith* antenna. Then, the adaptive weight in STAE is derived under the MMSE criterion, given by

$$\mathbf{w}_{ST} = \arg\min_{\tilde{\mathbf{w}}_{ST}} \left\| \mathbb{Y}\tilde{\mathbf{w}}_{ST} - \mathbf{s} \right\|^2, \quad (3)$$

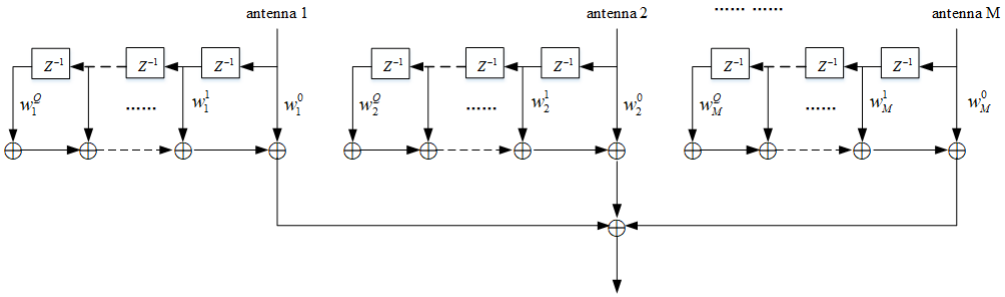

FIGURE 2. Illustration of space-time adaptive filtering in STAE.

where $\tilde{\mathbf{w}}_{ST}$ is the trial value of $\mathbf{w}_{ST}$. The optimal weights can be then directly obtained as

$$\mathbf{w}_{ST} = \mathbf{R}_{ST}^{-1}\mathbf{p}_{ST}, \tag{4}$$

where $\mathbf{R}_{ST} = \mathbb{Y}^H\mathbb{Y}$, $\mathbf{p} = \mathbb{Y}^H\mathbf{s}$ denotes auto-correlation matrix and cross-correlation vector, respectively.

Note that the concept of STAE has exhibited its powerful suppression ability for both multipath and multiuser interference [14], [19]. However, it can be observed that the main computation burden of (4) lies in the calculation of the autocorrelation matrix $\mathbf{R}_{ST}$ and its inversion. Note that $\mathbf{R}_{ST}$ is a common Hermitian matrix and of dimension $M(Q+1)\times M(Q+1)$. Hence, the calculation of optimal weight in STAE may suffer from high computational complexity, especially with a relative large temporal filter length Q.

III. ADAPTIVE SPACE-FREQUENCY CHANNEL EQUALIZATION

A. PROPOSED SPACE-FREQUENCY EQUALIZATION

The proposed SFAE employs the framework of frequency domain equalization, as illustrated in Fig. 3. We denote the *ith* time-domain data block received by the *mth* antenna as $\mathbf{y}_m^{(i)}$, and $\mathbf{y}_m^{(0)}$ corresponds to the pilot block. Each block is first transformed into frequency domain via discrete fourier transformation (DFT), i.e., $\mathbf{Y}_m^{(i)} = \mathbf{F}\mathbf{y}_m^{(i)}$. Here, $\mathbf{F}$ denotes the normalized DFT matrix. Then the frequency-domain signals are combined together by the carefully designed frequency-domain adaptive weights:

$$\mathbb{Y}^{(i)} = \sum_{m=1}^{M} \mathrm{diag}\left(\mathbf{Y}_m^{(i)}\right)\mathbf{W}_m = \sum_{m=1}^{M} \mathrm{diag}\left(\mathbf{F}\mathbf{y}_m^{(i)}\right)\mathbf{W}_m, \tag{5}$$

where $\mathbf{W}_m \in \mathbb{C}^{N\times 1}$ denotes the frequency-domain adaptive weight at the *mth* antenna. Transform $\mathbb{Y}^{(i)}$ into time domain through IDFT, and UW at the end of each block can be then removed.

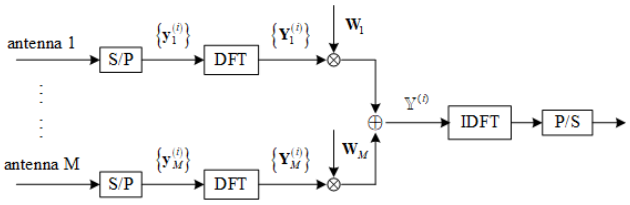

FIGURE 3. Illustration of frequency domain equalization in SFAE.

Denote the frequency-domain pilot as $\mathbf{S} = \mathbf{F}\mathbf{s}$. $\mathbf{W} = [\mathbf{W}_1^T, \mathbf{W}_2^T, \cdots, \mathbf{W}_M^T]^T$ is composed of the frequency-domain weights from all receiving antennas. Bear in mind that $\mathbb{Y}^{(0)}$ corresponds to the pilot block. According to MMSE criterion, the adaptive weight in frequency domain can be designed as

$$\begin{aligned}\mathbf{W} &= \arg\min_{\tilde{\mathbf{W}}} \left\| \mathbb{Y}^{(0)} - \mathbf{S} \right\|^2 \\ &= \arg\min_{\tilde{\mathbf{W}}} \left\| \sum_{m=1}^{M} \mathrm{diag}\left(\mathbf{Y}_m^{(0)}\right)\tilde{\mathbf{W}}_m - \mathbf{S} \right\|^2,\end{aligned} \tag{6}$$

where $\tilde{\mathbf{W}}_m$ denotes the trial value of $\mathbf{W}_m$.

If there is no further constraint among the elements of $\mathbf{W}_m$, we can directly decompose (6) into multiple subproblems at each subcarrier. Specifically, let $Y_m^{(0)}(k)$, $W_m(k)$ and $S(k)$ represent the kth element of $\mathbf{Y}_m^{(0)}$, $\mathbf{W}_m$ and $\mathbf{S}$, respectively. Denote $\mathbf{W}(k) = [W_1(k), W_2(k), \cdots, W_M(k)]^T$ and $\mathbf{Y}^{(0)}(k) = [Y_1^{(0)}(k), Y_2^{(0)}(k), \cdots, Y_M^{(0)}(k)]^T$. For $k = 0, 1, \cdots, N-1$, we can decompose (6) into

$$\begin{aligned}\mathbf{W}(k) &= \arg\min_{\tilde{W}_m(k)} \left\| \sum_{m=1}^{M} Y_m^{(0)}(k)\tilde{W}_m(k) - S(k) \right\|^2 \\ &= \arg\min_{\tilde{\mathbf{W}}(k)} \left\| \mathbf{Y}^{(0)}(k)^T\tilde{\mathbf{W}}(k) - S(k) \right\|^2.\end{aligned} \tag{7}$$

However, it is evident that the above estimation problem (7) falls in a underfitting problem, since for each subcarrier

$$\mathbb{Y} = \begin{bmatrix}\mathbf{Y}_1 & \mathbf{Y}_2 & \cdots & \mathbf{Y}_M\end{bmatrix} = \underbrace{\begin{bmatrix}\tilde{\mathbf{s}}_0 & \tilde{\mathbf{s}}_1 & \tilde{\mathbf{s}}_2 & \cdots & \tilde{\mathbf{s}}_{L+Q}\end{bmatrix}}_{N\times(L+Q+1)} \underbrace{\begin{bmatrix}\mathcal{T}(\mathbf{h}_1) & \mathcal{T}(\mathbf{h}_2) & \cdots & \mathcal{T}(\mathbf{h}_M)\end{bmatrix}}_{(L+Q+1)\times M(Q+1)} \tag{1}$$

$$\begin{aligned}\mathbf{Z}^{(0)} &= \mathbf{F}^H\mathbf{Y}^{(0)}\\ &= \mathbf{F}^H\left[\text{diag}\left(\mathbf{Y}_1{}^{(0)}\right)\mathbf{F}_Q \quad \text{diag}\left(\mathbf{Y}_2{}^{(0)}\right)\mathbf{F}_Q \quad \cdots\cdots \quad \text{diag}\left(\mathbf{Y}_M{}^{(0)}\right)\mathbf{F}_Q\right]\\ &= \left[\mathbf{F}^H\,\text{diag}\left(\mathbf{Y}_1{}^{(0)}\right)\mathbf{F}_Q \quad \mathbf{F}^H\,\text{diag}\left(\mathbf{Y}_2{}^{(0)}\right)\mathbf{F}_Q \quad \cdots\cdots \quad \mathbf{F}^H\,\text{diag}\left(\mathbf{Y}_M{}^{(0)}\right)\mathbf{F}_Q\right]\\ &= \underbrace{\left[\tilde{\mathbf{s}}_{-Q}\,\tilde{\mathbf{s}}_{-Q+1}\,\tilde{\mathbf{s}}_{-Q+2}\,\cdots\,\tilde{\mathbf{s}}_{L-1}\,\tilde{\mathbf{s}}_L\right]}_{N\times(L+Q+1)}\ \underbrace{\left[\mathcal{T}(\mathbf{h}_1)\,\mathcal{T}(\mathbf{h}_2)\,\cdots\,\mathcal{T}(\mathbf{h}_M)\right]}_{(L+Q+1)\times M(Q+1)}\end{aligned} \tag{12}$$

the $M\times 1$ weighting vector $\tilde{\mathbf{W}}(k)$ should be determined based on only one snapshot observation $\mathbf{Y}^{(0)}(k)$.

Based on the above observation, in SFAE, we introduce an additional time-domain constraint on the frequency-domain adaptive weights. Mathematically, let $\mathbf{F}_Q\in\mathbb{C}^{N\times(Q+1)}$ consist of the first and the last Q columns of $\mathbf{F}$. Then, because the number of time domain filter taps is finite, we assume the frequency-domain weight vector should satisfy the constraint of $\mathbf{W}_m=\mathbf{F}_Q\mathbf{w}_m$, where $\mathbf{w}_m\in\mathbb{C}^{(1+Q)\times 1}$. In other words, the time-domain vector corresponding to $\mathbf{W}_m$ should be only distributed within the $1+Q$ taps associated with $\mathbf{F}_Q$.

After substituting $\mathbf{W}_m$ with $\mathbf{F}_Q\mathbf{w}_m$, we can express adaptive space-frequency combination of the *ith* block as

$$\begin{aligned}\mathbb{Y}^{(i)} &= \sum_{m=1}^{M}\text{diag}\left(\mathbf{Y}_m^{(i)}\right)\mathbf{F}_Q\mathbf{w}_m\\ &= \underbrace{\left[\text{diag}\left(\mathbf{Y}_1^{(i)}\right)\mathbf{F}_Q \quad \cdots \quad \cdots \quad \text{diag}\left(\mathbf{Y}_M^{(i)}\right)\mathbf{F}_Q\right]}_{\mathbf{Y}^{(i)}\in\mathbf{C}^{N\times M(Q+1)}}\mathbf{w}\\ &= \mathbf{Y}^{(i)}\mathbf{w},\end{aligned} \tag{8}$$

where $\mathbf{w}=\left[\mathbf{w}_1^T,\mathbf{w}_2^T,\cdots,\mathbf{w}_M^T\right]^T$. Then, based on the pilot block, the time-domain vector can be obtained following the MMSE criterion:

$$\mathbf{w}=\arg\min_{\tilde{\mathbf{w}}}\left\|\mathbf{Y}^{(0)}\tilde{\mathbf{w}}-\mathbf{S}\right\|^2, \tag{9}$$

where $\tilde{\mathbf{w}}$ is the trial value of $\mathbf{w}$ and $\mathbf{Y}^{(0)}$ has been defined in (8). The optimal solution of $\mathbf{w}$ can be immediately obtained as

$$\mathbf{w}=\mathbf{R}^{-1}\mathbf{p}, \tag{10}$$

where the autocorrelation matrix and cross-correlation vector are expressed as $\mathbf{R}=\mathbf{Y}^{(0)H}\mathbf{Y}^{(0)}$ and $\mathbf{p}=\mathbf{Y}^{(0)H}\mathbf{S}$, respectively.

B. DISCUSSION ON INTERFERENCE SUPPRESSION

The proposed SFAE can suppress both the multipath interference from insufficient CP and the multiuser interference. In this subsection, we only take the multipath interference for example, whereas the following discussions can be easily extended to the case with multiuser interference.

We start by transferring (9) into its corresponding time-domain representation:

$$\mathbf{w}=\arg\min_{\tilde{\mathbf{w}}}\left\|\mathbf{Z}^{(0)}\tilde{\mathbf{w}}-\mathbf{s}\right\|^2, \tag{11}$$

where $\mathbf{Z}^{(0)}=\mathbf{F}^H\mathbf{Y}^{(0)}$ denotes the time-domain of $\mathbf{Y}^{(0)}$.

We first consider the situation without inter-block interference (with sufficient UW/CP). We can rewrite $\mathbf{Z}^{(0)}$ in the form of (12) on top of this page. Here, $\tilde{\mathbf{s}}_i$ denotes the downward cyclic shift of pilot $\mathbf{s}$ by a factor of i samples and $\mathcal{T}(\mathbf{h}_m)$ represents a Toeplitz matrix as shown in (2). It is observed that $\mathbf{Z}^{(0)}$ can be linearly represented by the column vectors of $\left[\tilde{\mathbf{s}}_{-Q},\tilde{\mathbf{s}}_{-Q+1},\tilde{\mathbf{s}}_{-Q+2},\cdots\tilde{\mathbf{s}}_{L-1},\tilde{\mathbf{s}}_L\right]$. Note that $\tilde{\mathbf{s}}_0$ corresponds to the expected pilot signal, and thus, the adaptive weight obtained from (11) targets at eliminating all the components of $\left[\tilde{\mathbf{s}}_{-Q},\tilde{\mathbf{s}}_{-Q+1},\tilde{\mathbf{s}}_{-Q+2},\cdots\tilde{\mathbf{s}}_{L-1},\tilde{\mathbf{s}}_L\right]$ except $\tilde{\mathbf{s}}_0$.

Then, we consider the situation with inter-block interference (with insufficient UW/CP). We assume the channel length is longer than the length of UW by a factor of P samples, i.e., $L=L_{UW}+P+1$, where L_{UW} is the length of UW.

For better presentation, we introduce the following $N\times(L+1)$ quasi-cyclic shift matrix:

$$\mathbf{X}=[\tilde{\mathbf{s}}_0,\tilde{\mathbf{s}}_1,\cdots,\tilde{\mathbf{s}}_{L_{UW}}\,\mathbf{x}^{(0)},\mathbf{x}^{(1)},\cdots\mathbf{x}^{(P)}], \tag{13}$$

where $\mathbf{x}^{(0)},\mathbf{x}^{(1)},\cdots\cdots,\mathbf{x}^{(P)}$ represent the quasi-cyclic shifts of $\tilde{\mathbf{s}}$ with the interference from previous block. Note that for the training block, the preamble serves as its previous block. Mathematically, we have

$$\begin{aligned}\mathbf{x}^{(0)} &= [x(0),s(-L_{UW}),s(-L_{UW}+1),\cdots s(0),\cdots\\ &\quad s(N-L_{UW}-2)]^T\in\mathbb{C}^{N\times 1}\\ \mathbf{x}^{(1)} &= [x(1),x(0),s(-L_{UW}),s(-L_{UW}+1),\cdots\\ &\quad s(0),\cdots s(N-L_{UW}-3)]^T\in\mathbb{C}^{N\times 1}\\ &\vdots\\ \mathbf{x}^{(P)} &= [x(P),\cdots x(1),x(0),s(-L_{UW}),s(-L_{UW}+1),\\ &\quad \cdots s(0),\cdots s(N-L_{UW}-2-P)]^T\in\mathbb{C}^{N\times 1},\end{aligned}$$

where $x(0)$ denotes the last symbol of the previous block, $x(1)$ denotes the second-to-last symbol, and so on.

We further denote $\tilde{\mathbf{X}}_i$ as the downward cyclic shift of $\mathbf{X}$ by a factor of i samples. Then, we can rewrite $\tilde{\mathbf{X}}_i$ for the following two cases:

When $i\le P$, we have

$$\tilde{\mathbf{X}}_{-i}=[\tilde{\mathbf{s}}_{-i},\cdots\tilde{\mathbf{s}}_{L_{UW}},\mathbf{x}^{(0)},\mathbf{x}^{(1)},\cdots\mathbf{x}^{(P-i)}]+\begin{bmatrix}\mathbf{0}_{(N-i)\times(L+1)}\\ *_{i\times(L+1)}\end{bmatrix}, \tag{14}$$

while for $i>P$, there holds

$$\tilde{\mathbf{X}}_{-i}=[\tilde{\mathbf{s}}_{-i},\tilde{\mathbf{s}}_{-i+1},\cdots,\tilde{\mathbf{s}}_{L_{UW}-(i-P)+1}]+\begin{bmatrix}\mathbf{0}_{(N-i)\times(L+1)}\\ *_{P\times(L+1)}\\ \mathbf{0}_{(i-P)\times(L+1)}\end{bmatrix}. \tag{15}$$

$$
\begin{aligned}
\mathbf{Z}^{(0)} &= \left[\mathbf{F}^H \operatorname{diag}\left(\mathbf{Y}_1{}^{(0)}\right)\mathbf{F}_Q \;\; \mathbf{F}^H \operatorname{diag}\left(\mathbf{Y}_2{}^{(0)}\right)\mathbf{F}_Q \;\; \cdots\cdots \;\; \mathbf{F}^H \operatorname{diag}\left(\mathbf{Y}_M{}^{(0)}\right)\mathbf{F}_Q\right] \\
&= \left[\tilde{\mathbf{x}}_{-Q}\begin{bmatrix} h_1(0) \\ h_1(1) \\ \vdots \\ h_1(L)\end{bmatrix} \tilde{\mathbf{x}}_{-Q+1}\begin{bmatrix} h_1(0) \\ h_1(1) \\ \vdots \\ h_1(L)\end{bmatrix} \cdots \mathbf{x}\begin{bmatrix} h_1(0) \\ h_1(1) \\ \vdots \\ h_1(L)\end{bmatrix} \cdots \tilde{\mathbf{x}}_{-Q}\begin{bmatrix} h_M(0) \\ h_M(1) \\ \vdots \\ h_M(L)\end{bmatrix} \tilde{\mathbf{x}}_{-Q+1}\begin{bmatrix} h_M(0) \\ h_M(1) \\ \vdots \\ h_M(L)\end{bmatrix} \cdots \mathbf{x}\begin{bmatrix} h_M(0) \\ h_M(1) \\ \vdots \\ h_M(L)\end{bmatrix}\right] \\
&= \underbrace{\left[\tilde{\mathbf{s}}_{-Q}\,\tilde{\mathbf{s}}_{-Q+1} \;\cdots\; \tilde{\mathbf{s}}_{L_{UW}-1}\;\tilde{\mathbf{s}}_{L_{UW}}\;\mathbf{x}^{(0)}\;\mathbf{x}^{(1)}\;\cdots\;\mathbf{x}^{(P)}\right]}_{N\times(L+Q+1)} \underbrace{\left[\mathcal{T}(\mathbf{h}_1)\;\mathcal{T}(\mathbf{h}_2)\;\cdots\;\mathcal{T}(\mathbf{h}_M)\right]}_{(L+Q+1)\times M(Q+1)} \\
&\quad + \begin{bmatrix}\mathbf{0}_{(N-Q)\times(L+1)} \\ *_{Q\times(L+1)}\end{bmatrix}\left[\mathbf{h}_1\otimes\mathbf{1}_{1\times(Q+1)}\;\mathbf{h}_2\otimes\mathbf{1}_{1\times(Q+1)}\;\cdots\;\mathbf{h}_M\otimes\mathbf{1}_{1\times(Q+1)}\right] \qquad (16)
\end{aligned}
$$

Here, we denote $*_{M\times N}$ as a $M \times N$ matrix whose elements may not be zeros. The detailed expressions for the elements of $*_{M\times N}$ are omitted for notational conciseness.

By using the definitions of $\tilde{\mathbf{X}}_{-i}$ in (14) and (15), we can finally rewrite $\mathbf{Z}^{(0)}$ in (16), as shown at the top of this page. It is observed that, the first term on the right hand side (RHS) of (16) falls into the similar model as (12) which corresponds to the situation without inter-block interference. We see that the first term can be linearly represented by the column vectors of $\left[\tilde{\mathbf{s}}_{-Q}, \tilde{\mathbf{s}}_{-Q+1}, \cdots \tilde{\mathbf{s}}_{L_{UW}-1}, \tilde{\mathbf{s}}_{L_{UW}}, \mathbf{x}^{(0)}, \mathbf{x}^{(1)}, \cdots \mathbf{x}^{(P)}\right]$ in which $\tilde{\mathbf{s}}_0$ corresponds to the expected pilot signal. Interestingly, the second term on the RHS of (16) is approximately a zero matrix. The only exception is that the last Q rows may not be zeros, which acts like interference. When $Q \ll N$, only a very small proportion of the rows will cause interference in $\mathbf{Z}^{(0)}$. Hence, in this case we can consider the second term on the RHS of (16) as a short burst interference. Note that once the above short burst interference has marginal contribution on the MMSE design in (11), the adaptive weight we obtained should have little capability to suppress this short interference in the last Q rows in $\mathbf{Z}^{(0)}$. This indicates that in the proposed SFAE, when there exists inter-block interference due to insufficient UW/CP, the last Q time-domain symbols in each block after equalization should still suffer from a certain burst interference and exhibit much lower SNR condition as compared to the rest $N - Q$ symbols.

Interestingly, we should emphasize that, as long as $Q \leq L_{UW}$, the above burst interference will be constrained only within the region of UW and will not influence any data symbols in the block. Hence, the proposed SFAE could work well with multipath interference in case of insufficient UW/CP in terms of data detection performance. Moreover, from the above discussions, we know in the absence of interference, the equalized data symbols and UW symbols will have equal SNR condition, while in case with interference, the equalized UW symbols will exhibit much lower SNR than the data symbols. The comparison between the SNR of equalized data and UW symbols can be employed to check the existence of interference. This is one unique property of the proposed SFAE method.

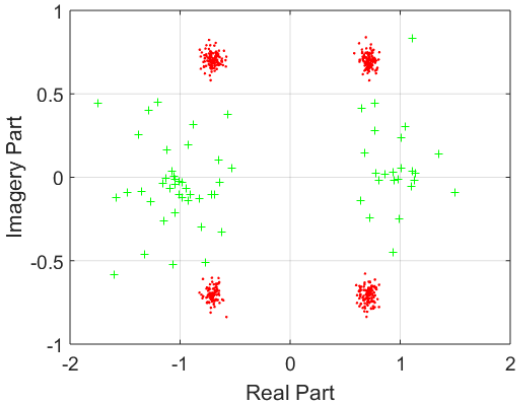

FIGURE 4. Constellation diagram of an equalized SFAE data block.

As an illustration example, in Fig. 4 we display one snapshot of the constellation diagram of an equalized SFAE data block. In this figure, we assume $Q = L_{UW} = 64$ and $N = 512$. The data symbols are drawn from QPSK while the UW symbols are drawn from BPSK. The red dots and green crosses represent the first $N - Q$ and last Q equalized symbols in the block, respectively. As expected, owing to the equivalent burst interference, we see that the last Q equalized symbols are distributed more dispersively. Moreover, Fig. 5 displays the corresponding energy from the first to the last symbols in the block. Due to the additional contribution of the introduced burst interference, the last Q symbols exhibit a sudden rise of energy as compared to the first $N-Q$ symbols. Once again, we should emphasize that, the resultant burst interference has been constrained within the UW region, and thus has no influence on the data detection.

C. COMPUTATIONAL COMPLEXITY ANALYSIS

The main computation burden of the proposed SFAE lies in the calculation of the autocorrelation matrix $\mathbf{R}$ and its inversion. Here we should note that, $\mathbf{R}$ in the proposed SFAE is composed of $M \times M$ submatrices, each of which is a standard Toeplitz matrix. Thus, the computation of $\mathbf{R}$ and its inversion have fast algorithms. It will be demonstrated that,

$$\mathbf{Y}^{(0)} = \left[\text{diag}\left(\mathbf{Y}_1{}^{(0)}\right)\mathbf{F}_Q \quad \text{diag}\left(\mathbf{Y}_2{}^{(0)}\right)\mathbf{F}_Q \quad \cdots\cdots \quad \text{diag}\left(\mathbf{Y}_M{}^{(0)}\right)\mathbf{F}_Q\right] = \left[\mathbf{B}_1 \quad \mathbf{B}_2 \quad \cdots\cdots \quad \mathbf{B}_M\right] \tag{17}$$

$$\begin{aligned}\mathbf{B}_i{}^H\mathbf{B}_j &= \mathbf{F}_Q{}^H \,\text{diag}\left(\mathbf{Y}_i{}^{(0)}\right)^H \text{diag}\left(\mathbf{Y}_j{}^{(0)}\right)\mathbf{F}_Q \\ &= \begin{bmatrix}\mathbf{f}_0{}^H \\ \mathbf{f}_1{}^H \\ \vdots \\ \mathbf{f}_Q{}^H\end{bmatrix}\begin{bmatrix}\mathbf{Y}_i{}^{(0)}(1)^H\mathbf{Y}_j{}^{(0)}(1) & 0 & \cdots & 0 \\ 0 & \mathbf{Y}_i{}^{(0)}(2)^H\mathbf{Y}_j{}^{(0)}(2) & \cdots & 0 \\ \vdots & \vdots & \ddots & \vdots \\ 0 & 0 & \cdots & \mathbf{Y}_i{}^{(0)}(N)^H\mathbf{Y}_j{}^{(0)}(N)\end{bmatrix}\left[\mathbf{f}_0 \quad \mathbf{f}_1 \quad \cdots \quad \mathbf{f}_Q\right]\end{aligned} \tag{19}$$

$$\begin{aligned}\mathbf{R}_{ij}(m,n) &= \mathbf{f}_m{}^H\begin{bmatrix}\mathbf{Y}_i{}^{(0)}(1)^H\mathbf{Y}_j{}^{(0)}(1) & 0 & \cdots & 0 \\ 0 & \mathbf{Y}_i{}^{(0)}(2)^H\mathbf{Y}_j{}^{(0)}(2) & \cdots & 0 \\ \vdots & \vdots & \ddots & \vdots \\ 0 & 0 & \cdots & \mathbf{Y}_i{}^{(0)}(N)^H\mathbf{Y}_j{}^{(0)}(N)\end{bmatrix}\mathbf{f}_n \\ &= \left[\mathbf{Y}_i{}^{(0)}(1)^H\mathbf{Y}_j{}^{(0)}(1) \quad \mathbf{Y}_i{}^{(0)}(2)^H\mathbf{Y}_j{}^{(0)}(2) \quad \cdots \quad \mathbf{Y}_i{}^{(0)}(N)^H\mathbf{Y}_j{}^{(0)}(N)\right]\mathbf{f}_{n-m}\end{aligned} \tag{20}$$

$$\mathbf{R}_{ij}(1,:) = \left[\mathbf{Y}_i{}^{(0)}(1)^H\mathbf{Y}_j{}^{(0)}(1) \quad \mathbf{Y}_i{}^{(0)}(2)^H\mathbf{Y}_j{}^{(0)}(2) \quad \cdots \quad \mathbf{Y}_i{}^{(0)}(N)^H\mathbf{Y}_j{}^{(0)}(N)\right]\left[\mathbf{f}_0 \quad \mathbf{f}_1 \quad \cdots \quad \mathbf{f}_Q\right] \tag{21}$$

the proposed SFAE should have much lower computational burden compared with the conventional STAE.

Specifically, we can rewrite $\mathbf{Y}^{(0)}$ given (17), as shown at the top of this page, $\mathbf{R}$ can be further expressed as

$$\begin{aligned}\mathbf{R} = \mathbf{Y}^{(0)H}\mathbf{Y}^{(0)} &= \begin{bmatrix}\mathbf{B}_1{}^H \\ \mathbf{B}_2{}^H \\ \vdots \\ \mathbf{B}_M{}^H\end{bmatrix}\left[\mathbf{B}_1 \quad \mathbf{B}_2 \quad \cdots \quad \mathbf{B}_M\right] \\ &= \begin{bmatrix}\mathbf{B}_1{}^H\mathbf{B}_1 & \mathbf{B}_1{}^H\mathbf{B}_2 & \cdots & \mathbf{B}_1{}^H\mathbf{B}_M \\ \mathbf{B}_2{}^H\mathbf{B}_1 & \mathbf{B}_2{}^H\mathbf{B}_2 & \cdots & \mathbf{B}_2{}^H\mathbf{B}_M \\ \vdots & \vdots & \ddots & \vdots \\ \mathbf{B}_M{}^H\mathbf{B}_1 & \mathbf{B}_M{}^H\mathbf{B}_2 & \cdots & \mathbf{B}_M{}^H\mathbf{B}_M\end{bmatrix}\end{aligned} \tag{18}$$

The detailed expression for the $(i,j)th$ subblock of $\mathbf{R}$, i.e., $\mathbf{R}_{ij} = \mathbf{B}_i{}^H\mathbf{B}_j$ is given in (19), as shown at the top of this page. Then, we will show that each matrix $\mathbf{R}_{ij}$ is a standard Toeplitz matrix. The $(m,n)th$ element of $\mathbf{R}_{ij}$ can be expressed in (20), as shown at the top of this page. It is evident that the elements $\mathbf{R}_{ij}(m,n)$ on k-diagonal $n = m + k$ are all equal to each other. That is to say, every submatrix of $\mathbf{R}$ is a standard Toeplitz matrix.

Next, we evaluate the computational burden of autocorrelation matrix and its inverse matrix in terms of complex multiplications for both the proposed SFAE and conventional STAE. In the proposed SFAE, since $\mathbf{R}_{ij}$ is a Toeplitz matrix, we only need to calculate its first row and first column. The first row of $\mathbf{R}_{ij}$ can be expressed in (21), as shown at the top of this page, which clearly indicates that the first row can be efficiently calculated by FFT. We can also make the similar observations for the first column of $\mathbf{R}_{ij}$. Moreover, based on the fact that $\mathbf{R}_{ij}$ is a Toeplitz matrix, after row and column permutations, $\mathbf{R}$ can be rewritten into a block Toeplitz matrix. The fast algorithm introduced in [21] can be then employed to calculate its inversion directly. In summary, we list the main computational burden of the proposed SFAE in Table 1. The results of the conventional STAE are also included for comparison, where the Cholesky decomposition is adopted to calculate the inversion of autocorrelation matrix.

Take $M = 4$, $Q + 1 = 64$ and $N = 512$ for example. We find that, the main computational burden of STAE is almost eight times as much as the proposed SFAE. As we will see in the later simulations, the proposed SFAE could perform similarly as STAE in terms of interference suppression. Hence, the proposed SFAE should be more attractive from practical point of view.

IV. SIMULATION

In this section, we evaluate the performance of the proposed SFAE in terms of uncoded bit error rate (BER). The conventional SC-FDE and STAE are also included for comparison. Unless otherwise stated, we consider that the number of receiving antennas is $M = 4$, $Q + 1 = 64$, the total block length and UW length are given by $N = 512$ and $L_{UW} = 64$, respectively. The pilot block is modulated by BPSK while the data blocks are modulated by QPSK. Both the cases with multipath and multiuser interference are evaluated.

TABLE 1. Multiplication quantities of R and its inversion.

Matrix	Multiplication quantity
$\mathbf{R}$ in STAE	$\frac{M(M+1)}{2}(N+Q-1)Q$
$\mathbf{R}$ in SFAE	$\frac{M(M+1)}{2}(N+N\log_2 N)+MN\log_2 N$
$\mathbf{R}^{-1}$ in STAE	$\frac{3}{2}[(MQ+M-1)(MQ+M-2)+\cdots+4\times 3]+3M^2(Q+1)^2-2M(Q+1)+16$
$\mathbf{R}^{-1}$ in SFAE	$(2Q+1)\{5M^2-M+3[(M-1)(M-2)+\cdots+2\times 1]\}+(4Q^2+8Q-2)M^3+2$

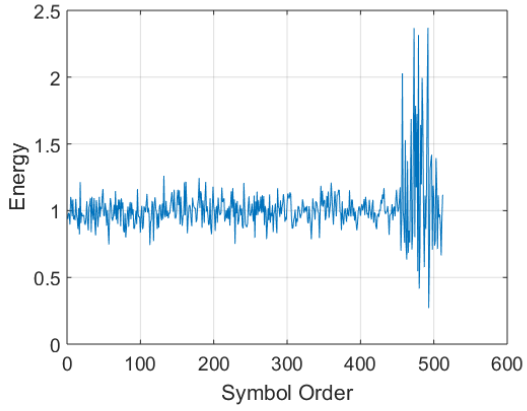

FIGURE 5. Signal energy of an equalized SFAE data block.

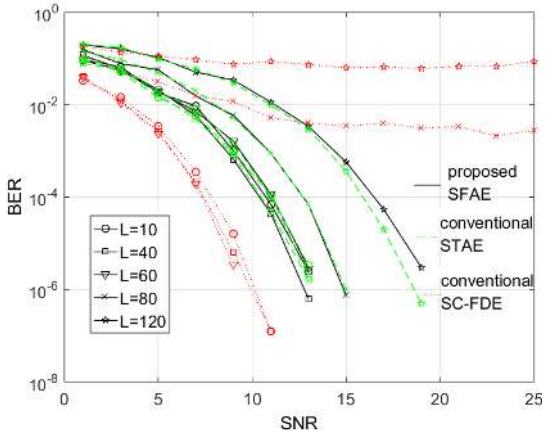

FIGURE 6. BER comparison between the proposed SFAE and conventional STAE and SC-FDE in the situation with insufficient UW/CP.

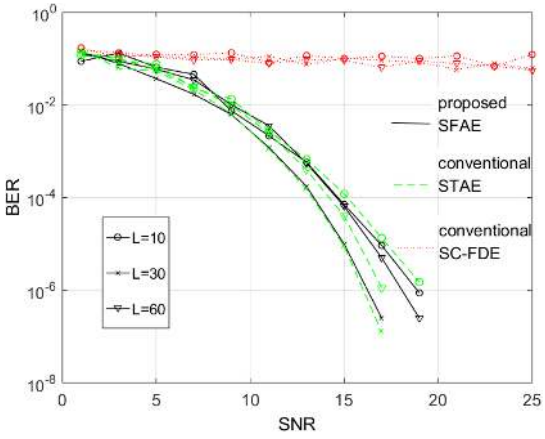

FIGURE 7. BER comparison between the proposed SFAE and the conventional STAE and SC-FDE with multiuser interference.

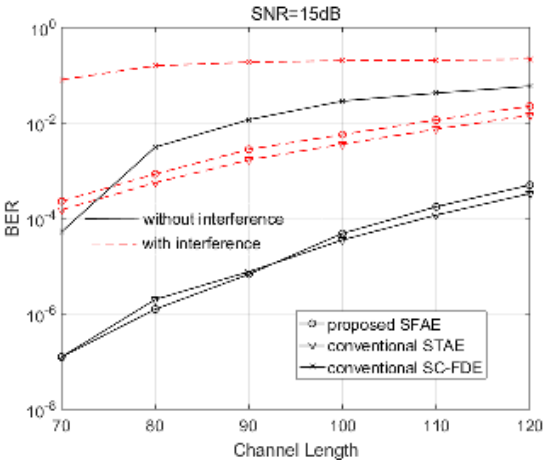

FIGURE 8. BER comparison with the channel length changes between the proposed SFAE, the conventional STAE and SC-FDE.

In Fig. 6, we show the BER comparison with different channel lengths between the proposed SFAE and conventional STAE and SC-FDE in the situation with insufficient UW/CP. The following observations can be made: When $L \leq L_{UW}$, i.e., with sufficient UW/CP, the BER performance of SC-FDE is the best among the three methods. However, once $L > L_{UW}$, i.e., with insufficient UW/CP, the SC-FDE fails to equalize the multipath effect and suffers from severe BER performance deterioration. In comparison, the conventional STAE and the proposed SFAE exhibit their robustness to the highly delay-dispersive channel, and could provide reliable channel equalization even if $L >> L_{UW}$. Moreover, it can be observed that the proposed SFAE behaves similarly as compared to the STAE.

In Fig. 7, we show the BER comparison between the proposed SFAE and conventional STAE and SC-FDE in the situation with multiuser interference. We consider that besides the expected transceivers, there is one concurrent interference link. The signal-to-interference ratio (SIR) is taken as 0 dB. It is seen that with multiuser interference, SC-FDE completely fails to decode properly due to its high vulnerability to interference. As expected, both STAE and the proposed SFAE have robustness to external multi-user interference and exhibit very close BER performance. Recalling that the proposed SFAE has much lower computational burden, we may conclude that the proposed SFAE would be more attractive from practical point of view.

In Fig. 8, we consider the BER comparison between the proposed SFAE and conventional STAE and SC-FDE with the channel length changes when SNR is given and $L > L_{UW}$. Let SNR = 15 dB. When with interference, let SIR = 0 dB. Whether without interference or with interference, the STAE and the proposed SFAE have good and steady BER performance with different channel lengths. For the SC-FDE, its BER performance is the worst among these three methods.

V. CONCLUSIONS

In this paper, we propose a SFAE method that can deal with both highly delay-dispersive channel and multiuser interference. The proposed adaptive weights can be derived through combining the received multi-antenna signals in frequency domain. The SFAE is more practical since it has a lower order of computational burden than the conventional STAE. The simulation results show that the proposed SFAE method has comparable interference suppression performance as the conventional STAE method.

REFERENCES

[1] O.-E. Barbu, C. N. Manchón, C. Rom, and B. H. Fleury, "Message-passing receiver for OFDM systems over highly delay-dispersive channels," *IEEE Trans. Commun.*, vol. 16, no. 3, pp. 1564–1578, Mar. 2017.
[2] E. Panayirci, H. Senol, and H. V. Poor, "Joint channel estimation, equalization, and data detection for OFDM systems in the presence of very high mobility," *IEEE Trans. Signal Process.*, vol. 58, no. 8, pp. 4225–4238, Aug. 2010.
[3] T. Pham, T. Le-Ngoc, G. Woodward, P. A. Martin, and K. T. Phan, "Equalization for MIMO-OFDM systems with insufficient cyclic prefix," in *Proc. IEEE VTC Spring*, Nanjing, China, May 2016, pp. 1–5.
[4] J.-B. Lim, C.-H. Choi, and G.-H. Im, "MIMO-OFDM with insufficient cyclic prefix," *IEEE Commun. Lett.*, vol. 10, no. 5, pp. 356–358, May 2006.
[5] T. Pham, P. A. Martin, G. Woodward, K. Prasad, and C. Horn, "Receiver design for SIMO-OFDM systems with insufficient cyclic prefix," in *Proc. IEEE 80th Veh. Technol. Conf.*, Vancouver, BC, Canada, Sep. 2014, pp. 1–5.
[6] M. Beheshti, M. J. Omidi, and A. M. Doost-Hoseini, "Equalisation of SIMO-OFDM systems with insufficient cyclic prefix in doubly selective channels," *IET Commun.*, vol. 3, no. 12, pp. 1870–1882, Dec. 2009.
[7] S. Chen and T. Yao, "FEQ for OFDM systems with insufficient CP," in *Proc. IEEE 14th Pers., Indoor Mobile Radio Commun.*, Sep. 2003, pp. 550–553.
[8] H. Lee, Y. Lee, and H. Park, "An efficient CP compensation for SC-FDE with insufficient CP symbols," *IEEE Commun. Lett.*, vol. 14, no. 6, pp. 548–550, Jun. 2010.
[9] A. Gusmao, P. Torres, R. Dinis, and N. Esteves, "A reduced-CP approach to SC/FDE block transmission for broadband wireless communications," *IEEE Trans. Commun.*, vol. 55, no. 4, pp. 801–809, Apr. 2007.
[10] H. Duan, X. Yu, and Y. Hou, "Efficient channel parameters estimation design for SC-FDE in HF wireless communications," in *Proc. 8th Int. Congr. Image Signal Process.*, Oct. 2015, pp. 1338–1342.
[11] W. Zhang, "Frequency synchronization for multi-user MIMO without cyclic-prefix based on space-time equalization," *IEEE Wireless Commun. Lett.*, vol. 6, no. 4, pp. 426–429, Aug. 2017.
[12] T. Tang and R. W. Heath, Jr., "Space-time interference cancellation in MIMO-OFDM systems," *IEEE Trans. Veh. Technol.*, vol. 54, no. 5, pp. 1802–1816, Sep. 2005.
[13] W. Zhang, H. Li, P. Mu, and W. Wang, "Robust multi-branch space–time beamforming for OFDM system with interference," *Digital Signal Process.*, vol. 65, pp. 63–70, Jun. 2017.
[14] T. Tang and R. W. Heath, Jr., "A space–time receiver with joint synchronization and interference cancellation in asynchronous MIMO-OFDM systems," *IEEE Trans. Veh. Technol.*, vol. 57, no. 5, pp. 2991–3005, Sep. 2005.
[15] M. B. Breinholt, M. D. Zoltowski, and T. A. Thomas, "Space-time equalization and interference cancellation for MIMO OFDM," in *Proc. 36th Asilomar Conf. Signals, Syst. Comput.*, vol. 2, Nov. 2002, pp. 1688–1693.
[16] R. Samanta, R. W. Heath, Jr., and B. L. Evans, "Joint space-time interference cancellation and channel shortening," in *Proc. Asil. Conf. Signals, Syst. Comput.*, Nov. 2003, pp. 32–36.
[17] R. Magueta, D. Castanheira, A. Silva, R. Dinis, and A. Gameiro, "Hybrid iterative space-time equalization for multi-user mmW massive MIMO systems," *IEEE Trans. Commun.*, vol. 65, no. 2, pp. 608–620, Feb. 2017.
[18] Z. Liu and G. B. Giannakis, "Space-time block-coded multiple access through frequency-selective fading channels," *IEEE Trans. Commun.*, vol. 49, no. 6, pp. 1033–1044, Jun. 2001.
[19] Y. Ge, W. Zhang, H. Wang, and F. Liu, "On adaptive length of temporal filter for space-time equalization with cochannel interference," *IEEE Signal Process. Lett.*, vol. 25, no. 7, pp. 999–1003, Jul. 2018.
[20] S. Zhou and G. B. Giannakis, "Space-time coding with maximum diversity gains over frequency-selective fading channels," *IEEE Signal Process. Lett.*, vol. 8, no. 10, pp. 269–272, Oct. 2001.
[21] H. Akaike, "Block Toeplitz matrix inversion," *SIAM J. Appl. Math.*, vol. 24, no. 2, pp. 234–241, 1973.

YAN LI received the B.S. degree from the School of Information Science and Engineering, Shandong University, Jinan, China, in 2017. She is currently pursuing the master's degree with the Ministry of Education Key Laboratory for Intelligent Networks and Network Security, Xi'an Jiaotong University. Her research interests include wireless communications and array signal processing.

WEILE ZHANG received the B.S. and Ph.D. degrees in information and communication engineering from Xi'an Jiaotong University, Xi'an, China, in 2006 and 2012, respectively. From 2010 to 2011, he was a Visiting Scholar with the Department of Computer Science, University of California at Santa Barbara, Santa Barbara, CA, USA. He is currently an Associate Professor with the Ministry of Education Key Laboratory for Intelligent Networks and Network Security, Xi'an Jiaotong University. His research interests include broadband wireless communications, MIMO, array signal processing, and localization in wireless networks.

RUIWEN JIANG received the B.S. degree from the School of Electronic and Information Engineering, Xi'an Jiaotong University, Xi'an, China, in 2016, where he is currently pursuing the master's degree with the Ministry of Education Key Laboratory for Intelligent Networks and Network Security. His research interests include wireless communications and equalization algorithm.

SHUN ZHANG received the B.S. degree in communication engineering from Shandong University, Jinan, China, in 2007, and the Ph.D. degree in communications and signal processing from Xidian University, Xi'an, China, in 2013, where he is currently with the State Key Laboratory of Integrated Services Networks. His research interests include MIMO-OFDM systems, relay networks, and detection and parameter estimation theory.